

Chemical-Scale Studies of the Phe-Pro Conserved Motif in the Cys Loop of Cys-Loop Receptors¹

2.1 Introduction

The Cys-loop superfamily of neurotransmitter-gated ion channels includes the nicotinic acetylcholine receptor (nAChR)², the 5-HT₃ serotonin receptor, the GABA_A and GABA_C receptors, and the glycine receptor (1, 2). Together, these receptors mediate both excitatory and inhibitory fast synaptic transmission throughout the central and peripheral nervous systems. The eponymous Cys loop, a disulfide-linked sequence Cys-Xaa₁₃-Cys, is located at the interface between the extracellular and transmembrane domains of the receptor (Figure 2.1A), and many studies have established that the Cys loop is essential for receptor function. Not part of the agonist binding-site, the Cys loop probably

¹ This chapter is a reproduced excerpt, with minor editing, from Limapichat, W.; Lester, H. A.; Dougherty, D. A. Chemical scale studies of the Phe-Pro conserved motif in the Cys loop of Cys loop receptors. *J. Biol. Chem.* **2010**, 285, 8976–8984. Copyright 2010 by the American Society of Biochemistry and Molecular Biology, Inc.

² The abbreviations used are: nAChR, nicotinic acetylcholine receptor; ACh, acetylcholine; SuCh, succinylcholine; Pip, pipecolic acid; Aze, azetidine-2-carboxylic acid; Dhp = 3,4-dehydroproline; Mor, morpholine-3-carboxylic acid; *c*-4F-Pro, *cis* 4-fluoro-proline, *t*-4F-Pro, *trans* 4-fluoro-proline; 3-Me-Pro, *trans* 3-methyl-proline; 2-Me-Pro, 2-methyl-proline; Cha, cyclohexylalanine; F-Phe, 4-fluorophenylalanine; F₃-Phe, 3,4,5-trifluorophenylalanine; Me-Pro, 4-Me-phenylalanine; Me₂-Phe, 3,5-dimethyl-phenylalanine; Fmoc, *N*-(9-fluorenyl)methoxycarbonyl; NVOC, *O*-nitroveratryloxycarbonyl; MS, mass spectrometry

plays a key role in receptor gating, transmitting structural changes initiated by agonist binding to the ion channel region of the receptor (3–7).

The intervening residues of the Cys loop show considerable conservation across the family (Figure 2.1B). Specifically, a completely conserved Phe-Pro motif (followed by Phe or Met) lies at the apex of the Cys loop. (These are residues 135 and 136 in the $\alpha 1$ subunit of the muscle-type nAChR, which is the system studied here.) Proline residues are unique among the 20 natural amino acids in several ways. Of particular interest here is the much greater tendency of prolyl peptide bonds to exist in the *cis* conformation (8–12). The presence of the Phe in the Phe-Pro motif makes this possibility more enticing. It is well established that an aromatic amino acid *N*-terminal of a proline enhances the likelihood of a *cis* conformation, roughly doubling the contribution of the *cis* peptide in the conformational equilibrium (12). Indeed, previous studies of the analogous motif in the 5-HT₃ receptor using conventional mutagenesis led to a postulation that the Pro was in a *cis* conformation (13).

Currently available structural information related to Cys-loop receptors adds to the intrigue (Figure 2.2). (Note that the acetylcholine-binding protein, arguably the most valuable structural model for the extracellular domain, does not contain a Cys loop and does not contain the Phe-Pro sequence (14).) In the medium resolution electron microscopic structure of the *Torpedo* nAChR (Protein Data Bank code 2BG9), the proline of the $\alpha 1$ subunit is in the *trans* conformation, and there is clearly no structural interaction at all between the side chains of Phe135 and Pro136 (15). In contrast, in the high-resolution x-ray crystal structure

of the mouse muscle nAChR α 1-subunit extracellular domain complexed to α -bungarotoxin (Protein Data Bank code 2QC1), the proline is in its *cis* form, and the Phe-Pro rings are stacked (16). (The *Torpedo* and mouse muscle receptors show very high sequence identity/similarity throughout their structures). Additionally, an NMR study of the isolated Cys loop of the nAChR found a roughly 1:1 mixture of *cis* and *trans* conformers, a ratio that can be modulated by glycosylation (17).

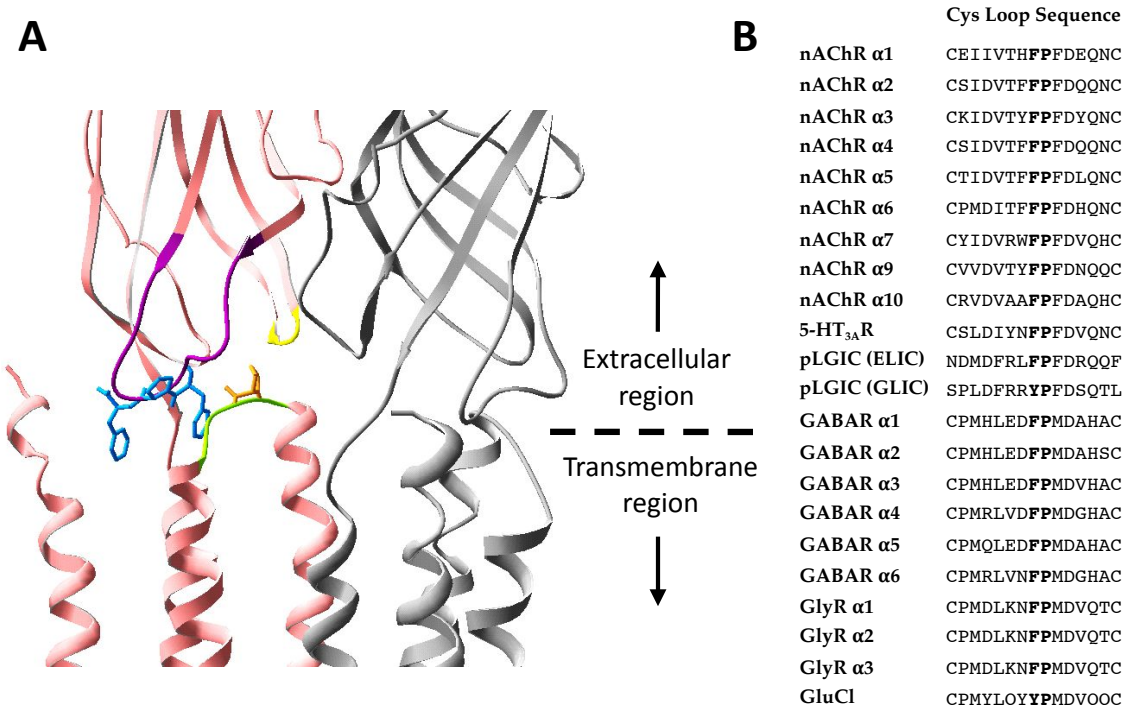


Figure 2.1. Topology of the Cys loop. **(A)** Structure of the extracellular and the transmembrane interface of the *Torpedo* nAChR (Protein Data Bank code 2BG9). Only the α -subunit (red) and the γ -subunit (grey) are shown. The Cys loop is highlighted in purple, $\beta 1$ - $\beta 2$ in yellow, and M2-M3 in green. The Phe-Pro-Phe motif in the Cys loop are shown in blue, and the Pro8* in the M2-M3 loop is shown in orange. **(B)** Sequence alignment of the Cys loop from various subunits of the Cys-loop superfamily

In recent years, several pentameric prokaryotic channels that are clearly related to the Cys-loop receptors have been discovered and crystallized. The prokaryotic channels contain a Phe/Tyr-Pro motif although they lack the cysteines of the Cys loop, and x-ray crystal structures confirm that the loop is still clearly in place. In a structure of the ELIC bacterial channel, which is believed to be a closed state (Protein Data Bank code 2VL0), the proline is in the *trans* conformation, and the Phe-Pro side chains are stacked (18). Two structures of the GLIC bacterial channel have appeared, and both are thought to be an open state of the channel. Both structures contain a completely stacked Tyr-Pro motif, but in one (Protein Data Bank code 3EAM), the proline is *cis* (19), and in the other (3EHZ) the proline is *trans* (20). The most recent crystal structure of the invertebrate glutamate-gated chloride channel from *C. elegans* (GluCl channel) reveals the Cys loops with a Tyr-Pro motif, and the proline appears to have the *trans* conformation (21).

Together, the structural data strongly indicate that (i) in the highly conserved Phe-Pro motif at the apex of the Cys loop of Cys-loop receptors, both *cis* and *trans* conformations around the prolyl amide bond are viable, and (ii) an interaction between the Phe and Pro side chains is possibly involved in the conformational preference. Although it is true that the three-dimensional fold of a protein may influence the *cis* preference of any given residue, the intrinsic conformational bias of the residue itself can still be expected to play an important role in determining structure and thus function of the protein (12).

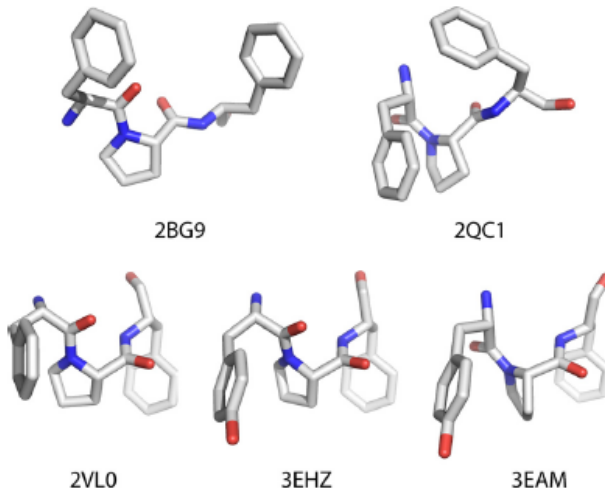


Figure 2.2. Images of the Phe/Tyr-Pro-Phe unit from five different relevant structures. Pro136 appears to have the *trans* conformation in the *Torpedo* nAChR (Protein Data Bank code 2BG9), ELIC bacterial channel (Protein Data Bank code 2VL0), and one GLIC bacterial channel (Protein Data Bank code 3EHZ) structures. However, crystal structures of the mouse muscle nAChR $\alpha 1$ -subunit extracellular domain (Protein Data Bank code 2QC1) and the other GLIC bacterial channel (Protein Data Bank code 3EAM) show Pro136 in the *cis* conformation.

The feasibility of both *cis* and *trans* conformations at Pro136 presents the tantalizing opportunity that *cis-trans* isomerization of this conserved proline in the Cys loop, facilitated by the adjacent Phe, might be involved in the receptor gating mechanism. Such a *cis-trans* isomerization at a different proline has been shown to be essential to channel gating in the 5-HT₃ receptor (5).

In the present work, we have used a variety of tools to probe the Phe-Pro motif of the muscle-type nAChR, including unnatural amino acid mutagenesis, electrophysiology, and NMR spectroscopy of model peptides. We find evidence for a strong interaction between the two residues and an important role for the aromatic nature of the Phe. At both sites, side-chain hydrophobicity is favorable

to the receptor function. In addition, the results reveal a correlation between receptor function and *cis* bias at the proline backbone across a simple homologous series of proline analogs. This suggests a significant role for the *cis* proline conformer at this site in receptor function.

2.2 Results

2.2.1 Mutational Studies at Pro136

A previous study of the muscle-type nAChR in HEK293 cells showed that P136G mutations in the β and γ subunits prevented receptor assembly, whereas analogous mutations in the α or δ subunits prevented trafficking of receptors to the cell surface (22). Similarly, in previous studies of the analogous proline in the homopentameric 5-HT₃ receptor, the P136A mutant revealed no surface expression in HEK293 cells (13). In the more permissive *Xenopus* oocyte expression system, the muscle-type nAChR containing the α P136A mutation produces < 10% of the current levels seen for wild type. Surprisingly, this mutant receptor has an ACh EC₅₀ value similar to that of the wild type. As discussed below, this result can be interpreted in several different ways; we therefore anticipated that the more subtle mutations enabled by unnatural amino acid mutagenesis would provide a more revealing analysis of the role of this residue.

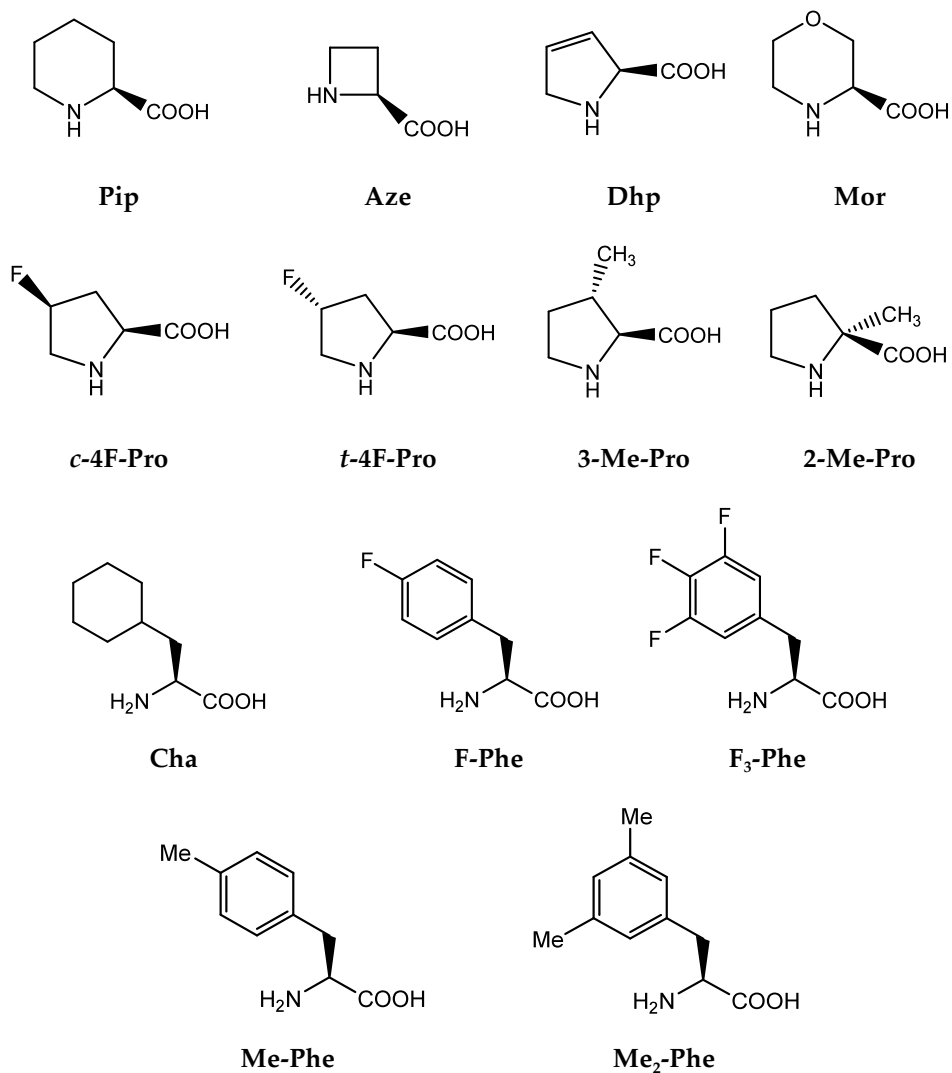


Figure 2.3. Structures of unnatural amino acids used in this study

Several unnatural analogs of proline (Figure 2.3) (5) were incorporated into the receptor using the *in vivo* nonsense-suppression method. These unnatural proline analogs have varying ring size, side-chain substitution, and intrinsic preferences for the *cis* conformer when probed in model systems (Table 2.1). The wild-type rescue experiment (i.e., incorporating Pro by nonsense suppression) displays the full phenotype of the wild-type receptor, including

ACh EC₅₀ value, Hill coefficient, and current traces. This indicates that the nonsense suppression methodology is viable at the 136 site. Interestingly, Pro analogues at position 136 are generally gain-of-function (lower EC₅₀), the sole exception being 2-Me-Pro, which gives essentially wild-type behavior. Similar to the Ala mutation mentioned above, the current levels from experiments involving 2-Me-Pro are < 10% of those seen in comparable experiments with other mutations. Despite the relative subtlety of the mutations, the gain-of-function effects can be substantial, as seen with Pip and 3-Me-Pro, which show 13- and 22-fold decreases in EC₅₀, respectively, relative to wild type.

Table 2.1. EC₅₀ and Hill constant values of mutant receptors containing unnatural amino acid at α 136

Residue α 136	Reported percentage cis ^a	ACh EC ₅₀	EC ₅₀ (mutant)/ EC ₅₀ (wild type)	Hill Constant	n
%		μ M			
Pro	5	23 \pm 0.2	1	1.5 \pm 0.02	35
Pro ^b	5	22 \pm 0.2	1	1.6 \pm 0.03	8
Pip	12	1.8 \pm 0.1	0.1	1.7 \pm 0.08	7
Aze	18	5.8 \pm 0.2	0.3	1.7 \pm 0.07	10
c-4F-Pro	~5	12 \pm 0.2	0.5	1.5 \pm 0.04	6
t-4F-Pro	~5	10 \pm 0.2	0.5	1.7 \pm 0.04	7
3-Me-Pro	~5	1.0 \pm 0.02	0.04	1.7 \pm 0.04	7
2-Me-Pro	0	25 \pm 0.7	1	1.6 \pm 0.06	10
Dhp	NR ^c	18 \pm 0.3	0.8	1.6 \pm 0.03	10
Mor	NR ^c	8.7 \pm 0.4	0.4	1.7 \pm 0.05	9

^aRef. (5,8)

^bData obtained by suppression mutation

^cNR, percentage cis values for these residues have not been reported in the literature.

Correlation between the *cis-trans* energy gap and the energy of channel activation could be expected if the receptor gating mechanism involves *cis-trans* isomerization of Pro136. However, no simple correlation is found (Table 2.1). For example, although both Pip and Aze show a stronger inherent *cis* preference than Pro and a lower EC₅₀, 3-Me-Pro shows a conformational bias very similar to that of Pro but a greatly diminished EC₅₀. Before analyzing these results in greater detail, however, we must consider the role of Phe135.

2.2.2 Mutational Studies at Phe135

Previous single channel studies have shown that the F135A mutation in the nAChR alters the gating mechanism, leading to two uncoupled open states that produce independent gating reactions from the diliganded closed state (23). In our studies of the nAChR, we found that the F135A mutation nearly obliterates receptor function; only very weak ACh-induced currents are observed despite normal surface expression levels (Figure 2.4).

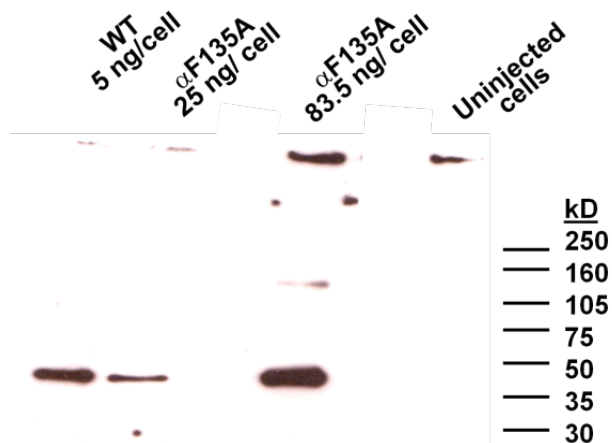


Figure 2.4. A Western blot analysis of Phe135Ala mutant receptor surface expression levels in comparison to the wild type. The experiment allowed visualization of the hemagglutinin epitope (HA) tag that had been incorporated into the α -subunit.

Seeking a more insightful analysis of the role of this residue, we probed the Phe135 site with an extensive series of Phe analogs. Again, the wild-type rescue experiment displays the full characteristics of the wild-type receptor. The Phe135 site is sensitive to even very subtle mutations, as shown in Table 2.2. Similar to what is observed with Pro136, Phe analogs consistently produce gain-of-function mutants. ACh sensitivity increases with the volume and number of hydrophobic substituents on the aromatic ring. For example, Me-Phe has a lower EC_{50} than F-Phe, and Me₂-Phe has a lower EC_{50} than Me-Phe. Surprisingly, cyclohexylalanine (Cha), which is similar to Phe in size and shape but is not aromatic (24), produces functional receptors with a small perturbation; EC_{50} is near the wild-type value. Given that the F135Cha mutant receptor is functional, aromaticity at position 135 is not an absolute requirement for the receptor to function.

To further explore the possible role of Phe135 in receptor gating, wild-type and mutant receptors were probed with the partial agonist succinylcholine (SuCh). Compared with ACh, SuCh produces only 14% of the maximal current under saturating drug concentrations in the wild-type receptor (Table 2.2). This indicates that upon receptor activation by SuCh, the channel open-closed equilibrium is shifted toward the open state, but to a much lesser extent relative to ACh activation. If a mutation produces a gain-of-function effect as a result of enhanced receptor gating, one could expect the mutation to improve the efficacy of a partial agonist like SuCh.

Table 2.2. EC₅₀ and Hill constant values of mutant receptors containing unnatural amino acid at α 135

Residue	ACh			SuCh			Efficacy ^a
	α 135	EC ₅₀	Hill Constant	<i>n</i>	EC ₅₀	Hill Constant	
μM							
Phe	23 ± 0.2	1.5 ± 0.02	35	59 ± 1	1.3 ± 0.03	13	0.14 ± 0.01
Phe ^b	23 ± 0.4	1.5 ± 0.03	8	NA ^c	NA ^c	NA ^c	NA ^c
F-Phe	2.6 ± 0.03	1.6 ± 0.02	7	32 ± 0.8	1.4 ± 0.04	9	0.54 ± 0.02
F ₃ -Phe	1.0 ± 0.02	1.5 ± 0.05	15	8.1 ± 0.2	1.6 ± 0.05	8	0.86 ± 0.02
Me-Phe	1.0 ± 0.02	1.6 ± 0.04	12	11 ± 0.2	1.5 ± 0.04	11	0.82 ± 0.02
Me ₂ -Phe	0.22 ± 0.01	1.6 ± 0.07	9	1.6 ± 0.06	1.5 ± 0.07	7	0.93 ± 0.04
Cha	16 ± 0.2	1.6 ± 0.02	15	60 ± 1	1.6 ± 0.03	9	0.10 ± 0.01

^a Determined by the average of I_{max}(SuCh)/I_{max}(ACh)

^b Data obtained by suppression mutation.

^c NA, data not available.

The EC₅₀ trend of SuCh (Table 2.2) parallels that of ACh, implying that the mutants respond to both drugs in the same way. As anticipated, all of the Phe

analogs that show a lowered EC_{50} do increase the relative efficacy of SuCh with respect to ACh. This suggests that mutations at position 135 primarily affect receptor gating. Note that the non-aromatic analog Cha shows essentially wild-type EC_{50} for both ACh and SuCh and that this mutation has no strong effect on the relative efficacy.

2.2.3 Interaction between Phe135 and Pro136

There is considerable evidence supporting a specific interaction in a Phe-Pro sequence that stabilizes the *cis* form of the Pro. This could possibly involve a polar- π interaction in which polarized C-H bonds ($C^{\delta-}H^{\delta+}$) on the proline interact favorably with the negative electrostatic potential on the face of the Phe side chain stacked on the Pro (9, 11). We investigated the possibility of a Phe-Pro interaction in this system by testing double mutant receptors in which Phe135 was substituted with the non-aromatic Cha and Pro136 was substituted with either Pip or 3-Me-Pro, the two mutations that cause the largest EC_{50} shifts. These experiments required consecutive incorporation of two different unnatural amino acids, an unprecedented experiment for receptors expressed in a living cell that was made possible by recent advances in tRNA design (25, 26). The resulting current signals (1–4 μ A) were quite sufficient for quantitative analysis.

The F135Cha mutation substantially diminishes the large effects of the mutations at Pro136. As shown in Figure 2.5, the 13- and 22-fold drops in EC_{50} for Pip and 3-Me-Pro, respectively, seen in a wild-type Phe background fall to ~

2.5-fold in the presence of F135Cha. A standard evaluation of double mutants employs a mutant cycle analysis, which has been used successfully with EC_{50} values for Cys-loop receptors in several instances (27–30). For the interaction of F135Cha with P136Pip and P136(3-Me-Pro), we find coupling parameters (Ω) of 5 and 10, respectively, which correspond to coupling energies ($RT\ln(\Omega)$) of 1.0 and 1.3 kcal/mol, respectively. These energies are significant for such subtle mutations and are indicative of a strong interaction between these two residues.

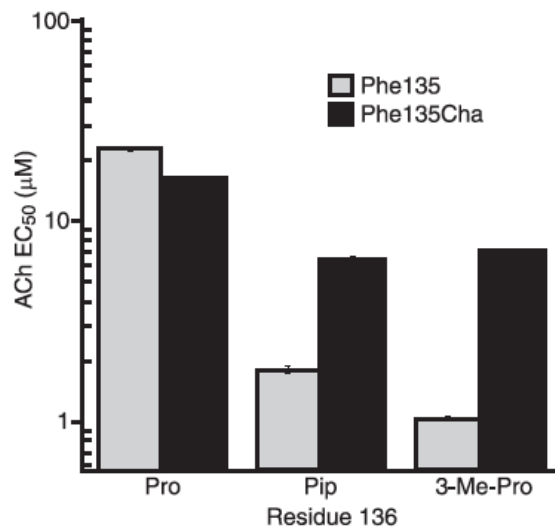


Figure 2.5. $ACh EC_{50}$ results from single and double mutation experiments at residues 135 and 136 in comparison with the wild-type value. For F135Cha/P136Pip, $EC_{50} = 6.5 \pm 0.2 \mu M$, Hill constant = $1.7 \pm 0.07 \mu M$, $n = 9$. For F135Cha/P135(3-Me-Pro), $EC_{50} = 6.9 \pm 0.2 \mu M$, Hill constant = $1.5 \pm 0.06 \mu M$, $n = 12$.

Having established a strong interaction between Phe135 and Pro136, we considered whether the intrinsic *cis-trans* equilibrium reported for proline and the proline analogs would be altered because of the preceding Phe. This would indicate that the percentage *cis* values used previously (31) and reported in Table

2.1 may not be appropriate for the present system because no aromatic amino acid was involved. As such, we set out to determine percentage *cis* values that are more appropriate to the Phe-Pro motif.

2.2.4 Determination of Inherent *cis* Preferences of Model Peptides Containing Proline Analogs Preceded by Phe

In order to determine whether the data in Table 2.1 reflect the innate *cis* preference of residue Pro136, it is necessary to measure the *cis-trans* energy gap ($\Delta G(c-t)$) for each unnatural amino acid substituted at this site, taking into account the aromatic–proline interaction. In fact, $\Delta G(c-t)$ for the Gly-Phe-Pro-Gly and Gly-Phe-Pip-Gly peptides have been reported (32). Using a similar solution NMR technique, it should be possible to determine $\Delta G(c-t)$ values for our series of unnatural analogs of proline following a Phe residue in model peptides.

Model peptides Gly-Phe- X_{Pro} -Gly, where X_{Pro} represents Pro, Pip, Aze, *c*-4F-Pro, Mor, 3-Me-Pro, and 2-Me-Pro, were synthesized via standard solid-phase peptide synthesis methods. These peptides were then subjected to solution NMR experiments similar to those in Ref. (32). Protons were assigned by two-dimensional gCOSY and/or TOCSY experiments. The proportion of each of the two conformers in solution was measured by integration of a corresponding, well-resolved peak after base-line correction. Representative sample spectra are shown in Figure 2.6. Conformational assignments were based on known chemical shifts of the Gly-Phe-Pip-Gly peptide reported in Ref. (32).

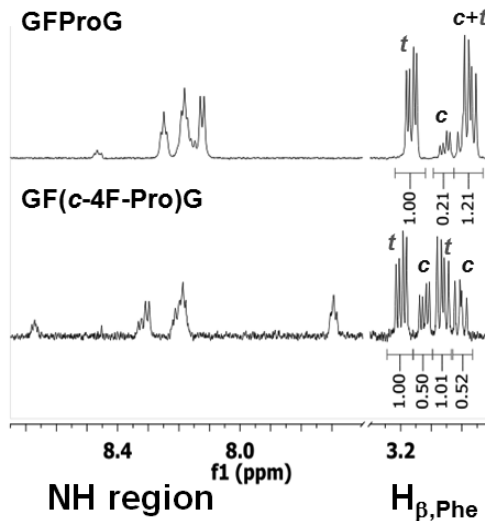


Figure 2.6. Samples of one-dimensional ^1H NMR spectra of Gly-Phe-Pro-Gly (top) and Gly-Phe-(*c*-4FPro)-Gly (bottom) peptides showing the amide and $\text{C}^\beta_{\text{Phe}}\text{H}_2$ regions. *t* denotes peaks from *trans* peptide. *c* denotes peaks from the *cis* peptide.

The results from the solution NMR experiments (Table 2.3) show that the *cis* preferences are indeed higher than the reported values in model peptides lacking the aromatic residue (Table 2.1). Note that for the Gly-Phe-(2-Me-Pro)-Gly peptide, the *cis* form was not observed. The model peptide containing Mor has a very high *cis* propensity; nearly 50% of the peptide is in the *cis* form. Moreover, one of the protons attached to the C^β of the Mor ring displays a large upfield shift in the *cis* peptide compared with that of the *trans* peptide (Table 2.4), as has also been reported with the structurally similar Pip (32). In the Pip-containing peptide, the chemical shifts of C^β protons are 1.72 and 2.15 ppm in the *trans* conformation and 0.35 and 1.90 ppm in the *cis* conformation. Likewise, for the Mor-containing peptide, the chemical shifts change from 3.74 and 4.37 ppm in the *trans* conformation to 2.10 and 3.74 ppm in the *cis* conformation. Most importantly, the

Phe residue can alter the trends in *cis-trans* preferences, as shown for the simple homologous series Aze, Pro, Pip (Table 2.1 compared with Table 2.3).

Table 2.3. $\Delta\Delta G(c-t)$ calculated from the percentage of *cis* results of solution NMR experiments for each amino acid and the $\Delta\Delta G(EC_{50})$ calculated from electrophysiology results of mutant receptors containing the corresponding amino acid at $\alpha 136$

X_{Pro}	Percentage <i>cis</i>	$\Delta\Delta G(c-t)^a$	$\Delta\Delta G(EC_{50})^b$
	%	(kcal.mol ⁻¹)	(kcal.mol ⁻¹)
Pro	17	0	0
Pip	39	0.65	1.5
Aze	30	0.42	0.81
<i>c</i> -4F-Pro	32	0.49	0.38
3-Me-Pro	12	-0.24	1.8
2-Me-Pro	0	-	-0.056
Mor	48	0.87	0.57

^a $\Delta\Delta G(c-t) = RT\ln(\% \text{ cis}(\text{Pro analogue}) / \% \text{ cis}(\text{Pro}))$.

^b $\Delta\Delta G(EC_{50}) = RT\ln(EC_{50}(\text{Pro analogue}) / EC_{50}(\text{Pro}))$.

Table 2.4. Proton chemical shift assignments in 90% H₂O/10% D₂O at pH 5, 298K for both the *trans* and the *cis* conformers of GAX_{Pro}G peptides

X _{Pro}		<i>trans</i>	<i>cis</i>
Pro	α	4.43	3.81
	β	1.96, 2.28	1.74, 1.93
	γ	2.00, 2.03	1.70, 1.73
	δ	3.58, 3.86	3.37, 3.53
Aze	α	NA ^{a,b}	3.96
	β	2.25, 2.60	2.10, 2.27
	γ	4.01, 4.36	3.73, 3.87
c-4F-Pro	α	4.68	3.91
	β	2.44, 2.54	1.70, 2.38
	γ	5.40	5.24
	δ	3.96, 4.05	3.66, 3.80
2-Me-Pro	-C ^α CH ₃	1.51	NA ^a
	β	1.98, 2.13	NA ^a
	γ	2.00, 2.03	NA ^a
	δ	3.71, 3.92	NA ^a
3-Me-Pro	α	4.00	3.54
	β	2.31	2.30
	-C ^β CH ₃	1.15	0.75
	γ	1.70, 2.17	1.31, 1.92
	δ	3.55, 3.90	3.26, 3.45
Pip	α	5.11	4.61
	β	1.72, 2.15	0.35, 1.90
	γ	1.46, 1.68	1.22, 1.44
	δ	1.55, 1.68	1.10, 1.58
	ε	3.20, 3.93	2.46, 4.32
Mor	α	5.00	4.40
	β	3.74, 4.37	2.10, 3.74
		3.90, 3.95	3.76, 4.06
	δ, ε ^c	3.47, 3.62	2.95, 3.10

^a NA, data not available

^b Possibly overlapping with the suppressed water peak

^c Unable to make a definite assignment

2.3 Discussion

Cys-loop neurotransmitter-gated ion channels are remarkable molecular machines. In response to the binding of a small-molecule ligand, these large proteins undergo a global conformational change, opening a selective ion channel and thereby converting a chemical event (i.e., ligand binding) to an electrical signal. The precise mechanism of this process is a central issue in molecular neurobiology. Recently, chemical-scale studies have provided valuable insights into the structure and function of these receptors, yet significant challenges still remain.

Here we have evaluated the highly conserved and structurally intriguing Phe135-Pro136 motif of the prototypic Cys-loop receptor, the nAChR. Proline is well appreciated to display novel conformational behaviors compared with all other natural amino acids. Additionally, it has been proposed that prolines might play a key role in the conformational changes that are essential to the function of many types of receptors (33). Several lines of evidence establish that local amino acids flanking proline can influence proline conformational preferences (9, 11, 12, 34). In particular, an aromatic residue preceding the proline is found to enhance the fraction of the *cis* isomer for peptides in solution (12). As shown in Figure 2.2, Pro136 can exist in both *cis* and *trans* conformations, and the two crystal structures with a *cis* peptide bond — the α 1 extracellular domain (Protein Data Bank code 2QC1) and the GLIC bacterial channel (Protein Data Bank code 3EAM) — show stacking of the Phe-Pro side chains. Given the complete conservation of the Phe-Pro motif and the available

structural data, it seemed reasonable to speculate that the *cis* conformer of Pro136 could be involved in receptor function.

Our primary measure of receptor function is EC₅₀, the effective concentration of agonist required to achieve half-maximal response. Agonist binding to a receptor induces step-by-step conformational changes that lead to opening of the ion channel; therefore, EC₅₀ is a value that reflects the composite effect of the agonist-binding affinity and the sequential gating events. The Phe-Pro motif is remote from the agonist-binding site, and the Cys loop is firmly established to play an essential role in gating (35). In addition, we find that a number of mutations at residue 135 greatly increase the efficacy of the partial agonist SuCh, supporting the notion that this residue participates in the gating mechanism. As such, we interpret changes in EC₅₀ to reflect primarily, if not exclusively, changes in receptor gating.

The involvement of the Phe-Pro motif in gating is further supported by a previous single channel study on the F135A mutation, which indicated that the gating mechanism is modified as a result of this mutation (23). The new mechanism appears to be much less efficient at coupling agonist binding to channel opening, consistent with our macroscopic observations of greatly reduced current for this mutant.

Conventional mutations at Pro136 also have strong effects on the receptor. When expressed in HEK293 cells, both Gly mutants in the nAChR subunits and an Ala mutant in the related 5-HT₃ receptor (13) gave receptors that were substantially impaired in the ability to assemble and/or traffic to the surface. In

the *Xenopus* oocyte system, we find that the P136A mutant gave < 10% of the current levels seen from wild type, again suggesting a disruption of assembly and/or trafficking or a disruption of gating.

Similarly, in an earlier study of Pro308 in the M2-M3 loop of the 5-HT₃ receptor, in which a compelling correlation between *cis* propensity of incorporated proline analogs and receptor function was demonstrated, structural disruption by conventional mutagenesis produced ambiguous results (5). In that study, Ala, Cys, Gly, Lys, Val, and Gln conventional mutants gave nonfunctional receptors. More recently, studies of an orthologous 5-HT₃ receptor showed that His and Trp mutants did give functional receptors (36). We note that aromatic amino acids, such as His and Trp, are more than twice as likely to be in a *cis* conformation as other non-proline natural amino acids (37). Again, the implications of the conventional mutagenesis results are open to debate.

Using conventional mutagenesis to probe the role of the *cis* conformation of a highly conserved proline is, in our view, unlikely to produce compelling results. Such studies frequently assume that simply seeing a functional receptor with a non-proline natural amino acid incorporated rules out a role for the *cis* conformer. However, previous studies have demonstrated that in some cases, when a *cis* proline is mutated to an alanine, the main-chain *cis* bond is preserved, presumably because the three-dimensional structure favors the *cis* conformation (11). In such cases, the Pro to Ala mutation often reduces the stability of the protein, which could manifest as lower expression levels, as we see with the P136A mutant. In addition, as with Pro, the presence of an aromatic amino acid

(such as Phe) N-terminal to an aliphatic residue (such as Ala) doubles the probability of a *cis* conformation (37). Alternatively, replacement of a proline with another natural amino acid could produce functional receptors via a different gating path that has become more energetically accessible, parallel to what is seen with the F135A mutation (23).

When studying such a structurally distinctive motif as Phe-Pro, the benefits of unnatural amino acid mutagenesis are amplified. The subtle perturbations allow one to maintain the essential motif while probing its intrinsic features. We have used unnatural amino acids to probe several aspects of the Phe-Pro motif, including the importance of Phe aromaticity, the roles of side-chain hydrophobicity and volume, and the possibility of *cis-trans* isomerization at the proline backbone.

Several intriguing observations emerge from the unnatural amino acid mutagenesis studies. Considering Pro136, subtle mutations produce noticeable changes in EC₅₀. For example, simply adding a methyl group (3-Me-Pro) can lower EC₅₀ 22-fold, and adding a single CH₂ group to the ring (Pip) can lower EC₅₀ 13-fold. Mutations are generally gain-of-function; EC₅₀ decreases. The only residue that is not gain-of-function but instead gives nearly wild-type EC₅₀ is 2-Me-Pro. Similar to Ala, 2-Me-Pro also produces much smaller whole cell currents.

As with the proline, subtle mutations of Phe135 can produce substantial changes in EC₅₀; a 100-fold shift arises from just the addition of two methyl groups fairly remote from the protein backbone (Me₂-Phe). Paralleling the

proline results, all of the unnatural amino acid mutants are gain-of-function. Moreover, an interesting trend is evident; Figure 2.7 shows a plot of $\log(EC_{50})$ for the receptor versus the side-chain $\log P$, a measure of its hydrophobicity. Although the cyclohexyl compound (Cha) is clearly an outlier, a significant correlation is seen among the aromatic side chains. These results indicate that hydrophobicity is an important determinant at position 135, with an increase in hydrophobicity making the channel easier to open. This is consistent with a molecular dynamics simulation of the $\alpha 7$ nAChR that places Phe135 in a hydrophobic pocket in an open state (38). In addition, the $\log P$ analysis (Figure 2.7) highlights the role of aromaticity at residue 135 because Cha has essentially the same hydrophobicity as both Me-Phe and F₃-Phe but a much higher EC_{50} . As such, the F135Cha mutant, being more hydrophobic than the wild-type Phe but lacking the aromaticity, appears to have a nearly wild-type ACh EC_{50} . From these data, we conclude that both hydrophobicity and aromaticity at position 135 are important in receptor function.

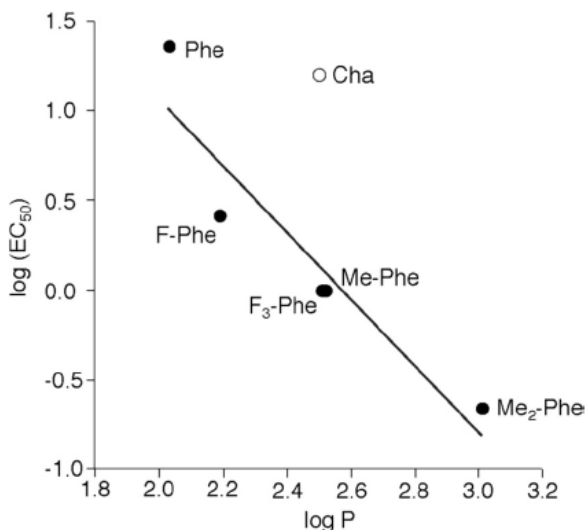


Figure 2.7. Correlation between EC_{50} and $\log P$ for mutations at Phe135. Note that the Cha point was not included in the linear fit.

The results of our double mutant studies have confirmed an important interaction between residues 135 and 136; the large effects caused by mutation at Pro136 are attenuated when Phe135 is simultaneously mutated to the non-aromatic Cha (Figure 2.5). Mutant cycle analysis shows significant coupling energies between residues 135 and 136.

We noted above the intriguing possibility that *cis-trans* isomerization at Pro136 is involved in receptor gating. In the present work, we did not see a simple correlation between EC_{50} and previously reported innate percentage *cis* values of the Pro analogs. However, there is ample precedent showing a deviation of percentage *cis* from the innate value when the preceding residue is aromatic (12). To probe the impact of the Phe residue on the present system, we used NMR spectroscopy to evaluate the *cis-trans* preference in the model peptides Gly-Phe- X_{Pro} -Gly, where X_{Pro} represents Pro, Pip, Aze, *c*-4F-Pro, Mor, 3-

Me-Pro, and 2-Me-Pro. Because the *cis* form of the Gly-Phe(2-Me-Pro)-Gly peptide was not observed, we cannot comment on the role of Phe in this system. In all other cases, comparisons are possible, and the Phe does increase the percentage *cis* at the adjacent Pro analog. The substantial upfield chemical shift of the C^β proton in the *cis* conformer supports the existence of the putative interaction between the proline ring and the aromatic ring of the phenylalanine residue (Table 2.4).

In Table 2.3, we report $\Delta\Delta G(c-t)$, the extent to which the proline analog shows an increased bias for the *cis* form relative to proline. To facilitate comparisons, we also convert each EC₅₀ shift into an energy term, $\Delta\Delta G(\text{EC}_{50})$. We first considered the homologous series of unsubstituted rings Aze, Pro, and Pip, in which the ring size expands from 4 to 5 to 6. The percentage *cis* and EC₅₀ values track each other; EC₅₀ is Pip < Aze < Pro, whereas percentage *cis* is Pip > Aze > Pro (Figure 2.8, solid line). Note that in this simple series, the Phe substituent is critical because the inherent percentage *cis* sequence absent the Phe is Aze > Pip > Pro (Figure 2.8, dotted line). Having an aromatic residue adjacent to the proline alters the *cis* bias differentially across this homologous series, and the EC₅₀ values for the receptor mirror this effect. These data suggest that proline *cis-trans* isomerization at this site may play a role in receptor gating.

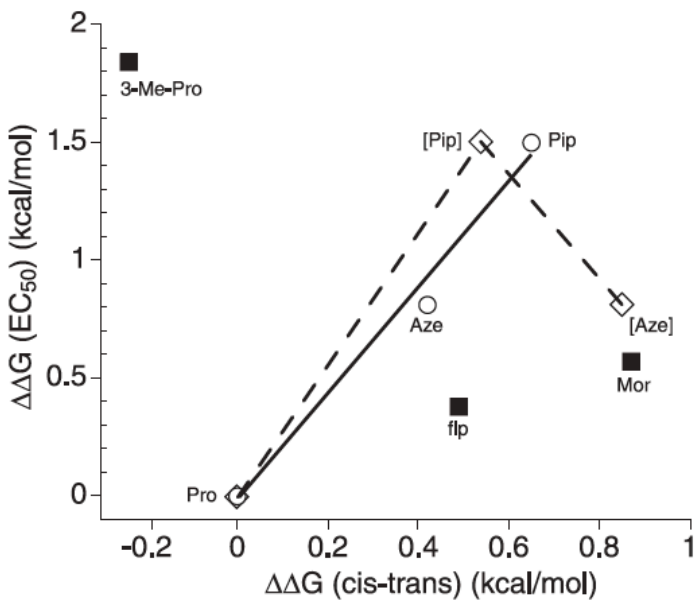


Figure 2.8. Relationship between EC_{50} values and *cis-trans* preferences for Pro and analogs at position 136. All values are relative to Pro. Solid line and open circles, Pro, Aze, and Pip using *cis-trans* values determined in the present study for the Gly-Phe-Xaa-Gly sequence (Table 2.3). Dashed line and open diamonds, Pro, Aze, and Pip using *cis-trans* values previously determined for sequences that do not have an aromatic N-terminal to the Pro analog. Solid squares, data points (*c*-4F-Pro, Mor, and 3-Me-Pro) that deviate from the trend set by the solid line

Concerning the more dramatic proline mutations, a simple percentage *cis* correlation is not evident. It is clear from the Phe135 mutational studies that receptor function is highly sensitive to side-chain polarity at the 135 site (Figure 2.7), with increased side-chain hydrophobicity lowering EC_{50} . It seems reasonable to expect a similar effect at the adjacent Pro136 because Phe and Pro interact, as shown by the mutant cycle analysis. Indeed, our results suggest a preference for side-chain hydrophobicity at the Pro136 site as well. Mor is structurally very similar to Pip, but it does not fit into the Aze-Pro-Pip correlation. We propose that EC_{50} for Mor is anomalously high because of the increased polarity relative to Pip. Similarly, *c*-4F-Pro has a significantly higher percentage *cis* than Pro but

only a modest decrease in EC_{50} , apparently due to the increased polarity of the fluorine substituent. In fact, a second linear correlation can be seen in Figure 2.8 involving the Pro-(*c*-4F-Pro)-Mor series, although the structural variation across this series is less consistent than in the Aze-Pro-Pip trio. 3-Me-Pro shows a smaller percentage *cis* than Pro but the lowest EC_{50} among the amino acids at the 136 sites. Interestingly, adding a single CH_3 group to Pro136 has the same effect on EC_{50} as adding a single CH_3 group to Phe135 (3-Me-Pro and Me-Phe show the same EC_{50}). Inspection of simple molecular models leads to an observation that the two CH_3 groups could point into nearly the same region of the receptor when the proline is in the *cis* form. Perhaps each CH_3 fits into a hydrophobic pocket, stabilizing the open state of the receptor and lowering EC_{50} .

As shown Figure 2.8, in the most conservative structural series (Pro, Pip, and Aze), we do find a trend that is suggestive of *cis-trans* isomerization at Pro136. Importantly, this trend is seen only when the perturbing effect of the Phe residue is included, justifying the consideration of the Phe-Pro unit as a single motif. Residues that involve more complex changes do not fit the correlation, but generally the deviation is consistent with the notion that increasing side-chain hydrophobicity lowers EC_{50} . From our data, we propose that both *cis* propensity and side-chain hydrophobicity at Pro136 simultaneously are determinants of nAChR function. Moreover, the possibility of *cis-trans* isomerization at Pro136 being involved in gating cannot be ruled out.

In summary, the subtle mutations enabled by unnatural amino acid mutagenesis have allowed a detailed study of the Phe-Pro motif in the Cys loop

of a Cys-loop receptor. Mutant cycle analysis reveals a strong interaction between the two residues and a strong preference for an aromatic residue at position 135. In addition, a clear trend is evident whereby increasing hydrophobicity at either Phe135 or Pro136 lowers EC₅₀. Although the analysis of residue Pro136 is complex, the data provide evidence supporting a role of the *cis* conformer in receptor function.

2.4 Materials and Methods

Synthesis of dCA-amino acids

The preparations of amino acids coupled to the dinucleotide (dCA) have been described previously (39) with the exception of dCA-Dhp and dCA-Mor. (S)-3-morpholinecarboxylic acid HCl was purchased from Tyger Scientific, Inc. (Ewing, NJ), and 3,4-dehydro-*L*-proline (Dhp) from Chem-Impex International Inc. (Wood Dale, IL). The amino groups were protected as the *O*-nitroveratryloxycarbonyl (NVOC) group. NVOC-Cl was purchased from Aldrich. (NVOC)-3,4-dehydroproline cyanomethyl ester and (NVOC)-morpholine cyanomethyl ester were prepared according to the representative protocol reported in Ref. (40). Products were characterized by NMR spectroscopy. The NMR spectra, both ¹H and ¹³C, are complicated because each compound shows two distinct conformations in the solution.

(NVOC)-3,4-Dehydroproline cyanomethyl ester. ¹H NMR (500 MHz, CDCl₃) 83.95–4.03 (m, 6H), 4.34–4.43 (m, 2H), 4.69–4.87 (m, 2H), 5.20–5.21 (m, 2H), 5.43–

5.67 (m, 2H), 5.76–5.83 (m, 1H), 7.01 (s, 1H), 7.71 (m, 1H). ^{13}C NMR (125 MHz, CDCl_3) δ 49.20, 49.23, 53.57, 54.20, 56.54, 56.57, 56.87, 64.66, 65.08, 65.92, 66.28, 108.34, 108.37, 110.07, 111.25, 113.96, 113.98, 123.46, 123.71, 127.44, 127.85, 130.37, 130.49, 139.88, 139.92, 148.32, 148.43, 153.39, 153.76, 153.81, 153.96, 168.41, 168.83. High-resolution MS analysis (FAB $^+$) calcd for $\text{C}_{17}\text{H}_{18}\text{N}_3\text{O}_8$ m/z = 392.1094, found 392.1109.

(NVOC)-Morpholine cyanomethyl ester. ^1H NMR (500 MHz, CDCl_3) δ 3.24–3.48 (m, 1H), 3.51 (dt, 1H), 3.69–3.75 (m, 1H), 3.83–3.95 (m, 2H), 3.94–3.95 (m, 3H), 3.99–4.02 (m, 3H), 4.33–4.41 (m, 1H), 4.63–4.85 (m, 3H), 5.41 (dd, 1H), 5.69 (dd, 1H), 6.88–6.97 (m, 1H), 7.66–7.70 (m, 1H). ^{13}C NMR (125 MHz, CDCl_3) δ 41.22, 41.73, 49.39, 49.45, 54.53, 55.05, 56.53, 56.60, 56.81, 64.91, 65.31, 66.29, 66.73, 66.99, 67.34, 108.32, 108.36, 109.91, 111.13, 113.84, 113.89, 126.93, 127.66, 139.78, 140.11, 148.32, 148.53, 153.66, 153.81, 155.14, 156.04, 168.69, 168.89. High-resolution MS analysis (FAB $^+$) calcd for $\text{C}_{17}\text{H}_{20}\text{N}_3\text{O}_9$ m/z = 410.1199, found 410.1180.

Dhp and Mor cyanomethyl esters were coupled to dCA following the protocol in Ref. (40).

dCA-Dhp. ES-MS calcd for $\text{C}_{34}\text{H}_{40}\text{N}_{10}\text{O}_{20}\text{P}_2$ m/z 970.2; found (M - H) $^-$ m/z 969.0, (M+Na-2H) $^-$ m/z 991.1, and (M+Na-H) $^-$ m/z 992.0.

dCA-Mor. ES-MS calcd for $\text{C}_{34}\text{H}_{42}\text{N}_{10}\text{O}_{21}\text{P}_2$ m/z 988.2; found (M - H) $^-$ m/z 987.0, (M+Na-2H) $^-$ m/z 1009.0, and (M+Na-H) $^-$ m/z 1010.0.

Molecular Biology

Subunits of embryonic mouse muscle nAChR were in pAMV vectors. The α subunit contains the hemagglutinin epitope (HA) tag in the M3-M4 loop. There is no significant shift in EC₅₀ caused by the insertion of the HA tag at this location. Site-directed mutagenesis was performed using the Stratagene QuikChange protocol. For single unnatural amino acid incorporation, the site of interest was mutated to an amber stop codon. For double unnatural acid incorporation, the 135 site was mutated to the opal stop codon and the 136 site was mutated to the amber stop codon. Circular cDNA was linearized with NotI or KpnI. After purification (Qiagen), linearized DNA was used as a template for runoff *in vitro* transcription using T7 mMessage mMachine kit (Ambion). The resulting mRNA was purified (RNAeasy Mini Kit, Qiagen) and quantified by UV-visible spectroscopy.

THG73 (41) and TQOpS' (25, 26) were used as amber suppressor tRNA and opal suppressor tRNA, respectively. Conjugated dCA-amino acid was ligated to 74-nucleotide tRNA as previously reported (39). Crude tRNA-amino acid product was used without desalting, and the product was confirmed by MALDI-TOF MS on 3-hydroxypicolinic acid (3-HPA) matrix. Deprotection of the NVOc group on tRNA-amino acid was carried out by 5-minute photolysis immediately prior to injection.

Microinjection

Stage V–VI *Xenopus laevis* oocytes were employed. For wild-type receptor and receptors containing conventional mutations, quantified mRNA of all subunits were mixed in a ratio of $\alpha:\beta:\gamma:\delta = 2:1:1:1$ by mass. If an unnatural amino acid was to be incorporated into the α subunit, the mRNA stoichiometry was $\alpha:\beta:\gamma:\delta = 10:1:1:1$ by mass. Total amount of injected mRNA was 0.5–5 ng per cell for the wild type, 5–50 ng per cell for conventional mutations, and 25–125 ng per cell for suppression mutations. More mRNA was used in the double mutation experiments and with some mutations that gave abnormally low expression level. Equal volumes of the mRNA mixture and unprotected tRNA–amino acid were mixed prior to injection. Approximately 15ng of tRNA per cell was used in the single suppression experiments and 50 ng in the double suppression experiments. Each oocyte was injected with 50 nL of RNA solution, and cells were incubated for 18–72 hours at 18 °C in culture media (ND96⁺ with 5% horse serum). In the case of low-expressing mutant receptors, a second injection was required. As a negative control for all suppression experiments, 76-nucleotide tRNA (dCA ligated to 74-nucleotide tRNA) was co-injected with mRNA in the same manner as fully charged tRNA.

Western blot analysis

The injected oocytes were incubated for 48 hours in ND96⁺ with 5% horse serum. The vitelline/plasma membranes were isolated by physical dissection after the oocytes were incubated in hypotonic solution (5 mM HEPES, 5 mM NaCl) with 50 µL membrane solubilization solution (50 mM Tris, pH 7.5, 10 mM EDTA, 4% SDS w/v, 1mM phenanthroline, 10 µM pepstatin A) for 10 minutes. Following 5-minute centrifugation at 4 °C and removal of the supernatant, the pellets were mixed with 10 µL smashing buffer (4.7 µL of exchange buffer (100 mM NaCl, 50 mM Tris, pH 7.9), 300 µL 10% SDS, 89 mg DDM, and 1 protease inhibitor tablet) and 10 µL of 2x loading buffer. The experiment was performed using SDS-PAGE with 15% Tris-Cl ReadyGels (BioRad Laboratories). 10 oocytes were used in each lane. The samples were subjected to a Western blot analysis using antihemagglutinin antibody, and visualized using an ECL detection kit (Amersham).

Electrophysiology

Acetylcholine chloride and succinylcholine dihydrate were purchased from Sigma-Aldrich/RBI. Drug dilutions were prepared from 1M stock solutions in the calcium-free ND96 buffer.

Ion channel function in oocytes was assayed by current recording in two-electrode voltage-clamp mode using the OpusXpress 6000A (Axon Instruments). For dose-response experiments, 1 mL of each drug solution was applied to the

cells, and between 12 and 16 concentrations of drug were used. Oocytes were clamped at -60 mV. Cells were perfused in calcium-free ND96 solution at flow rates of 1 mL/min before agonist application, 4 mL/min during agonist application, and 3 mL/min during wash. Drug application was 15 seconds in duration. Data were sampled at 125 Hz and filtered at 50 Hz.

Data Analysis

All dose-response data were obtained from at least 5 cells and at least two batches of oocytes. Data were normalized ($I_{max} = 1$) and averaged. EC_{50} and Hill coefficient (n_H) were determined by fitting averaged, normalized dose-response relations to the Hill equation. Dose-responses of individual oocytes were also examined and used to determine outliers. Individual dose-response data with $n_H > 2$ or $n_H < 1$ were discarded.

Coupling parameter (Ω) between any two mutations at residue 135 and 136 was calculated from Equation 1,

$$\Omega = [EC_{50}(\text{double mutation}) \times EC_{50}(\text{wild type})] / [EC_{50}(135 \text{ mutation}) \times EC_{50}(136 \text{ mutation})] \quad (\text{Eq.1})$$

Side chain logP values were obtained using the ChemDraw program (CambridgeSoft Corporation).

Synthesis of Fmoc-Protected Amino Acid

Fmoc-Cl was purchased from Fluka. (S)-3-morpholinecarboxylic acid HCl was purchased from Tyger Scientific, Inc. (Ewing, NJ), (2S,3S)-3-methylpyrrolidine-2-carboxylic acid (3-Me-Pro) from Acros Organics USA (Morris Plains, NJ), α -methyl-L-proline (2-Me-Pro) from Fluka, and 3,4-dehydro-L-proline (Dhp) from Chem-Impex International, Inc. (Wood Dale, IL). The amino acids were coupled to the Fmoc protecting group using the following protocol.

L-amino acid (0.06 mmol) was dissolved in 10% Na_2CO_3 in water (2 mL), resulting in a solution with pH \sim 9. To this solution was added Fmoc-Cl (1.5 eq) in dioxane (2 mL) at room temperature. DIPEA was added dropwise while the reaction was stirred. Typically, the reaction was complete within 6 hours. The reaction mixture was diluted by addition of brine (20 mL). This was extracted with ether (5 mL) 5 times. The aqueous layer was acidified with 6 N HCl to pH of \sim 1 (solution became cloudy), and extracted with ether (5 mL) 3 times or until the organic layer was clear. The combined organic layers were dried over Na_2SO_4 , and the solvent was removed under reduced pressure. Crude product was dried under vacuum overnight and was used in the next step (solid-phase peptide synthesis) without further purification.

N-Fmoc-2-methyl-proline. ^1H NMR (500 MHz, CDCl_3) δ 1.26–1.62 (m, 3H), 1.75–1.98, (m, 3H), 2.15–2.42 (m, 1H), 3.51–3.63 (m, 2H), 4.13–4.56 (m, 3H), 7.27–7.41 (m, 4H), 7.55–7.61 (m, 2H), 7.70–7.77 (m, 2H). ^{13}C NMR (125 MHz, CDCl_3) δ 22.31, 22.72, 22.83, 23.42, 39.23, 41.11, 47.48, 47.58, 48.28, 48.91, 65.00, 66.28, 67.25, 67.65,

120.12, 120.20, 124.92, 124.95, 125.30, 125.35, 127.27, 127.29, 127.30, 127.74, 127.78, 127.93, 141.54, 141.56, 141.60, 141.62, 144.05, 144.17, 144.21, 144.43, 154.86, 155.35, 178.42, 179.54. High-resolution MS analysis (FAB⁺) calcd for C₂₁H₂₂NO₄ m/z = 352.1549, found 352.1534.

N-Fmoc-3-methyl-proline. ¹H NMR (500 MHz, CDCl₃) δ 1.17–1.28 (m, 3H), 1.49–1.63 (m, 1H), 2.01–2.15 (m, 1H), 2.40–2.49 (m, 1H), 3.50–3.68 (m, 2H), 3.85–3.97 (m, 1H), 4.12–4.28 (m, 1H), 4.33–4.46 (m, 2H), 7.27–7.40 (m, 2H), 7.53–7.62 (m, 2H), 7.69–7.77 (m, 2H). ¹³C NMR (125 MHz, CDCl₃) δ 18.65, 18.91, 31.58, 32.50, 38.24, 39.70, 45.92, 46.29, 47.27, 47.30, 65.59, 66.07, 67.72, 67.77, 119.94, 119.97, 120.04, 125.05, 125.11, 125.16, 125.24, 127.10, 127.13, 127.15, 127.68, 127.78, 127.79, 141.27, 141.34, 141.36, 141.39, 143.80, 143.84, 144.07, 144.12, 154.75, 155.46, 176.79, 177.69. ESI MS on an LCQ ion trap mass spectrometer (positive ion mode) calcd for C₂₁H₂₁NO₄ m/z = 351.1, found 351.9.

N-Fmoc-morpholine. ¹H NMR (500 MHz, CDCl₃) δ 3.04–3.92 (m, 6H), 4.20–4.68 (m, 5H), 7.27–7.34 (m, 2H), 7.36–7.42 (m, 2H), 7.48–7.60 (m, 2H), 7.71–7.77 (m, 2H). ¹³C NMR (125 MHz, CDCl₃) δ 41.16, 41.73, 47.27, 54.45, 54.84, 66.37, 66.75, 67.32, 67.72, 67.77, 68.12, 120.11, 120.14, 124.79, 124.89, 125.13, 127.19, 127.25, 127.27, 127.86, 127.90, 141.37, 141.42, 141.45, 141.48, 143.78, 143.82, 143.94, 155.91, 156.58, 174.83, 175.02. ESI MS on an LCQ ion trap mass spectrometer (positive ion mode) calcd for C₂₀H₁₉NO₅Na m/z = 376.1, found 376.3.

Solid-phase peptide synthesis

All peptides were synthesized by solid-phase methods from Fmoc-protected amino acids using HBTU (Fluka) as a coupling reagent. Fmoc-*L*-proline (Fmoc-Pro) was purchased from Sigma, Fmoc-*L*-pipecolic acid (Fmoc-Pip) from Peptech Corporation (Burlington, MA), Fmoc-*L*-Azetidine-2-carboxylic acid (Fmoc-Aze) from Fluka, Fmoc-*cis*-2-fluoro-*L*-proline (Fmoc-*c*-4F-Pro) from AnaSpec, Inc. (San Jose, CA), *N*-Fmoc-glycine (Fmoc-Gly) from Aldrich, and Fmoc-*L*-phenylalanine (Fmoc-Phe) from Sigma. All chemicals were used as purchased without purification.

PAL resin (Sigma-Aldrich, estimated 0.4–0.8 mmol/g loading, 1 % cross-linked with divinylbenzene, 100–200 mesh) was used to afford carboxy terminal primary amides. For conventional amino acids, couplings were performed with 3 equivalents of Fmoc amino acid, 3 equivalents of HBTU, and 6 equivalents of diisopropylethylamine (DIPEA). For unnatural amino acids, couplings were performed with 2 equivalents of Fmoc amino acid, 2 equivalents of HBTU, and 4 equivalents of DIPEA. The reaction time for each coupling step was 1-2 hours. Kaiser test was performed to monitor the progress of the reaction. After each coupling step, unreacted free amine was acetylated (5% acetic anhydride and 5% pyridine, and 90% DMF) for 8 minutes, followed by deprotection of Fmoc-protected amine groups (20% piperidine/DMF, 15 minutes). In the last step, after Fmoc deprotection, the peptides were acetylated at the *N*-termini on the resin using a solution of 5% pyridine, 5% acetic anhydride, and 90% DMF. Peptides were cleaved from the resin by treatment with trifluoroacetic acid (TFA)

and water (95:5) for 2 hours. After filtration to collect the filtrate, solvents were removed as much as possible under reduced pressure. Following addition of 5% acetic acid solution, this solution was lyophilized to dryness. The peptides were purified by preparative-scale reversed-phase high-pressure liquid chromatography (HPLC) with gradient elution using an A-B gradient (buffer A 0.05% TFA in water; buffer B 20% water and 0.05% TFA in acetonitrile) and the flow rate of 15 mL/min. Peptide identity was characterized by ESI MS on an LCQ ion trap mass spectrometer (positive ion mode).

GFProG (M+Na)⁺ expected 440.2, observed 440.3.

GF(2-Me-Pro)G (M+Na)⁺ expected 454.2, observed 454.3.

GF(3-Me-Pro)G (M+Na)⁺ expected 454.2, observed 454.4.

GF(c-4F-Pro)G (M+Na)⁺ expected 458.2, observed 458.4.

GFAzeG (M+Na)⁺ expected 426.2, observed 426.2.

GFPipG (M+Na)⁺ expected 454.2, observed 454.3.

GFMorG (M+Na)⁺ expected 456.2, observed 456.2.

Note that the synthesis of Gly-Phe-Dhp-Gly peptide did not give the desired product in the first trial, and no further attempt has been made to obtain the product.

NMR Spectroscopy of Model Peptides

The peptide samples were dissolved in 5mM phosphate buffer with 25 mM NaCl in 90% H₂O/10% D₂O at pH 5. Samples for NMR experiments were between 2 and 5 mM. NMR spectra were acquired on a Varian 600 MHz spectrometer, and the temperature was set to 298 K. The water signal was suppressed by presaturation. Sequential assignments were achieved using gradient selected correlated spectroscopy (gCOSY) and total correlation spectroscopy (TOCSY) experiments. Spectra were all internally referenced to 3-(trimethylsilyl) propionic-2,2,3,3-*d*₄ acid sodium salt (TSP, ~ 200 μM final concentration) at 0.0 ppm. The fraction of *cis* conformer was determined by integrating well-resolved peaks in the one-dimensional ¹H NMR spectra. NMR data were processed using the MestReNova software version 5.1.0 (Mestrelab Research S. L.).

2.6 Supplemental Figure

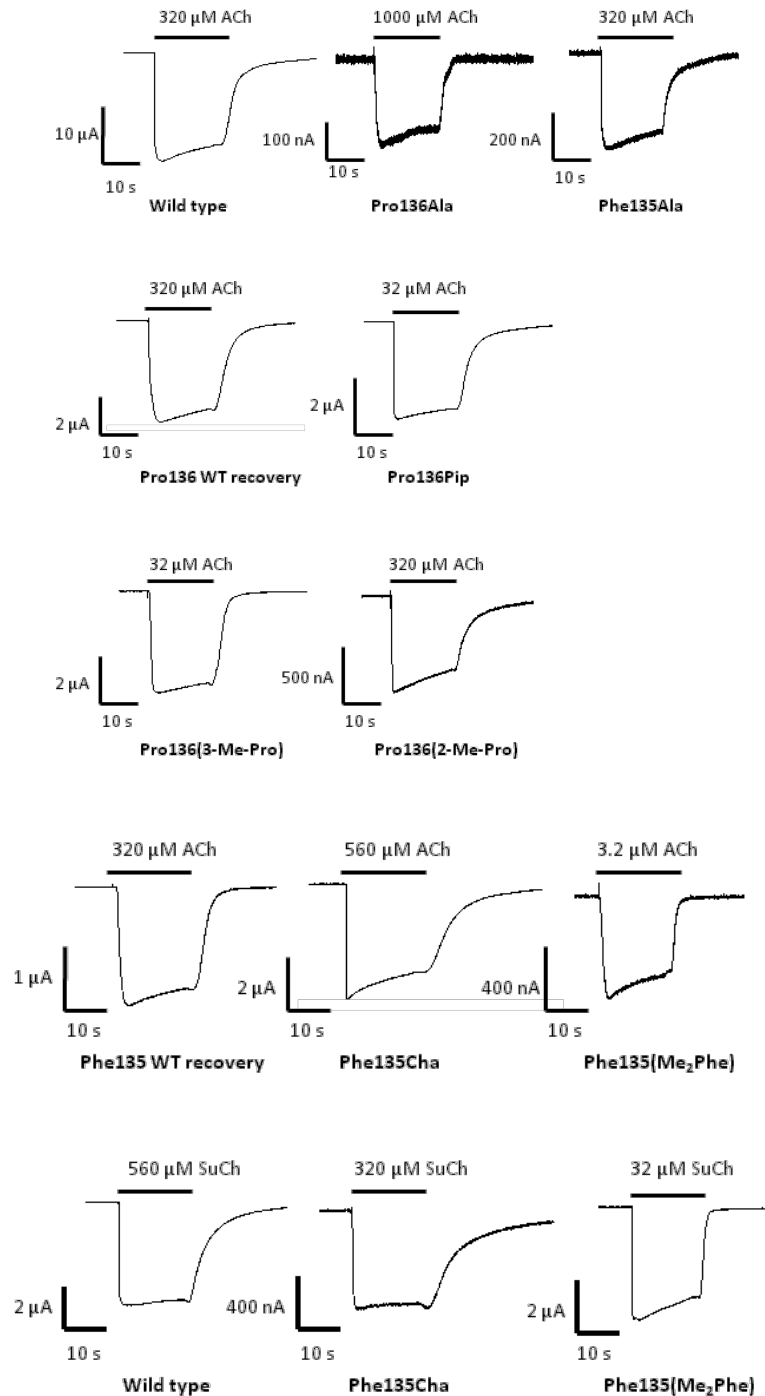


Figure 2.S1. Sample current traces from wild-type and mutant nAChR at saturating doses of ACh or SuCh

2.7 Acknowledgments

We thank Dr. Scott A. Ross for help with the NMR experiments and Professor Sarah C. R. Lummis for helpful discussion.

2.8 References

- (1) Corringer, P. J.; Le Novère, N.; Changeux, J. P. Nicotinic receptors at the amino acid level. *Annu. Rev. Pharmacol. Toxicol.* **2000**, *40*, 431–458.
- (2) Grutter, T.; Changeux, J. P. Nicotinic receptors in wonderland. *Trends Biochem. Sci.* **2001**, *26*, 459–463.
- (3) Bouzat, C.; Gumilar, F.; Spitzmaul, G.; Wang, H. L.; Rayes, D.; Hansen, S. B.; Taylor, P.; Sine, S. M. Coupling of agonist binding to channel gating in an ACh-binding protein linked to an ion channel. *Nature* **2004**, *430*, 896–900.
- (4) Karlin, A. Emerging structure of the nicotinic acetylcholine receptors. *Nat. Rev. Neurosci.* **2002**, *3*, 102–114.
- (5) Lummis, S. C. R.; Beene, D. L.; Lee, L. W.; Lester, H. A.; Broadhurst, R. W.; Dougherty, D. A. Cis-trans isomerization at a proline opens the pore of a neurotransmitter-gated ion channel. *Nature* **2005**, *438*, 248–252.
- (6) Millar, N. S. Assembly and subunit diversity of nicotinic acetylcholine receptors. *Biochem. Soc. Trans.* **2003**, *31*, 869–874.
- (7) Jha, A.; Cadigan, D. J.; Purohit, P.; Auerbach, A. Acetylcholine receptor gating at extracellular transmembrane domain interface: the cys-loop and M2–M3 linker. *J. Gen. Physiol.* **2007**, *130*, 547–558.
- (8) Dugave, C.; Demange, L. Cis-trans isomerization of organic molecules and biomolecules: implications and applications. *Chem. Rev.* **2003**, *103*, 2475–2532.
- (9) Bhattacharyya, R.; Chakrabarti, P. Stereospecific interactions of proline residues in protein structures and complexes. *J. Mol. Biol.* **2003**, *331*, 925–940.
- (10) MacArthur, M. W.; Thornton, J. M. Influence of proline residues on protein conformation. *J. Mol. Biol.* **1991**, *218*, 397–412.
- (11) Pal, D.; Chakrabarti, P. Cis peptide bonds in proteins: residues involved, their conformations, interactions and locations. *J. Mol. Biol.* **1999**, *294*, 271–288.

- (12) Reimer, U.; Scherer, G.; Drewello, M.; Kruber, S.; Schutkowski, M.; Fischer, G. Side-chain effects on peptidyl-prolyl cis/trans isomerisation. *J. Mol. Biol.* **1998**, *279*, 449–460.
- (13) Deane, C. M.; Lummis, S. C. The role and predicted propensity of conserved proline residues in the 5-HT₃ receptor. *J. Biol. Chem.* **2001**, *276*, 37962–37966.
- (14) Brejc, K.; van Dijk, W. J.; Klaassen, R. V.; Schuurmans, M.; van Der Oost, J.; Smit, A. B.; Sixma, T. K. Crystal structure of an ACh-binding protein reveals the ligand-binding domain of nicotinic receptors. *Nature* **2001**, *411*, 269–276.
- (15) Unwin, N. Refined structure of the nicotinic acetylcholine receptor at 4 Å resolution. *J. Mol. Biol.* **2005**, *346*, 967–989.
- (16) Dellisanti, C. D.; Yao, Y.; Stroud, J. C.; Wang, Z.-Z.; Chen, L. Crystal structure of the extracellular domain of nAChR alpha1 bound to alpha-bungarotoxin at 1.94 Å resolution. *Nat. Neurosci.* **2007**, *10*, 953–962.
- (17) Rickert, K. W.; Imperiali, B. Analysis of the conserved glycosylation site in the nicotinic acetylcholine receptor: potential roles in complex assembly. *Chem. Biol.* **1995**, *2*, 751–759.
- (18) Hilf, R. J. C.; Dutzler, R. X-ray structure of a prokaryotic pentameric ligand-gated ion channel. *Nature* **2008**, *452*, 375–379.
- (19) Bocquet, N.; Nury, H.; Baaden, M.; Le Poupon, C.; Changeux, J.-P.; Delarue, M.; Corringer, P.-J. X-ray structure of a pentameric ligand-gated ion channel in an apparently open conformation. *Nature* **2009**, *457*, 111–114.
- (20) Hilf, R. J. C.; Dutzler, R. Structure of a potentially open state of a proton-activated pentameric ligand-gated ion channel. *Nature* **2009**, *457*, 115–118.
- (21) Hibbs, R. E.; Gouaux, E. Principles of activation and permeation in an anion-selective Cys-loop receptor. *Nature* **2011**, *474*, 54–60.
- (22) Fu, D. X.; Sine, S. M. Asymmetric contribution of the conserved disulfide loop to subunit oligomerization and assembly of the nicotinic acetylcholine receptor. *J. Biol. Chem.* **1996**, *271*, 31479–31484.
- (23) Chakrapani, S.; Bailey, T. D.; Auerbach, A. Gating dynamics of the acetylcholine receptor extracellular domain. *J. Gen. Physiol.* **2004**, *123*, 341–356.
- (24) McMenimen, K. A.; Dougherty, D. A.; Lester, H. A.; Petersson, E. J. Probing the Mg²⁺ blockade site of an N-methyl-D-aspartate (NMDA) receptor with unnatural amino acid mutagenesis. *ACS Chem. Biol.* **2006**, *1*, 227–234.

- (25) Rodriguez, E. A.; Lester, H. A.; Dougherty, D. A. Improved amber and opal suppressor tRNAs for incorporation of unnatural amino acids in vivo. Part 1: minimizing misacylation. *RNA* **2007**, *13*, 1703–1714.
- (26) Rodriguez, E. A.; Lester, H. A.; Dougherty, D. A. Improved amber and opal suppressor tRNAs for incorporation of unnatural amino acids in vivo. Part 2: evaluating suppression efficiency. *RNA* **2007**, *13*, 1715–1722.
- (27) Kash, T. L.; Jenkins, A.; Kelley, J. C.; Trudell, J. R.; Harrison, N. L. Coupling of agonist binding to channel gating in the GABA_A receptor. *Nature* **2003**, *421*, 272–275.
- (28) Price, K. L.; Millen, K. S.; Lummis, S. C. R. Transducing agonist binding to channel gating involves different interactions in 5-HT₃ and GABA_C receptors. *J. Biol. Chem.* **2007**, *282*, 25623–25630.
- (29) Venkatachalan, S. P.; Czajkowski, C. A conserved salt bridge critical for GABA_A receptor function and loop C dynamics. *Proc. Natl. Acad. Sci. U.S.A.* **2008**, *105*, 13604–13609.
- (30) Gleitsman, K. R.; Kedrowski, S. M. A.; Lester, H. A.; Dougherty, D. A. An intersubunit hydrogen bond in the nicotinic acetylcholine receptor that contributes to channel gating. *J. Biol. Chem.* **2008**, *283*, 35638–35643.
- (31) Lummis, S. C.; Beene, D. L.; Lee, L. W.; Lester, H. A.; Broadhurst, R. W.; Dougherty, D. A. Cis-trans isomerization at a proline opens the pore of a neurotransmitter-gated ion channel. *Nature* **2005**, *438*, 248–252.
- (32) Wu, W.-J.; Raleigh, D. P. Conformational heterogeneity about pipecolic acid peptide bonds: conformational, thermodynamic, and kinetic aspects. *J. Org. Chem.* **1998**, *63*, 6689–6698.
- (33) Sansom, M. S.; Weinstein, H. Hinges, swivels and switches: the role of prolines in signalling via transmembrane alpha-helices. *Trends Pharmacol. Sci.* **2000**, *21*, 445–451.
- (34) Thomas, K. M.; Naduthambi, D.; Zondlo, N. J. Electronic control of amide cis-trans isomerism via the aromatic-prolyl interaction. *J. Am. Chem. Soc.* **2006**, *128*, 2216–2217.
- (35) Sine, S. M.; Engel, A. G. Recent advances in Cys-loop receptor structure and function. *Nature* **2006**, *440*, 448–455.
- (36) Paulsen, I. M.; Martin, I. L.; Dunn, S. M. J. Isomerization of the proline in the M2-M3 linker is not required for activation of the human 5-HT_{3A} receptor. *J. Neurochem.* **2009**, *110*, 870–878.
- (37) Jabs, A.; Weiss, M. S.; Hilgenfeld, R. Non-proline cis peptide bonds in proteins. *J. Mol. Biol.* **1999**, *286*, 291–304.

- (38) Cheng, X.; Ivanov, I.; Wang, H.; Sine, S. M.; McCammon, J. A. Nanosecond-timescale conformational dynamics of the human alpha7 nicotinic acetylcholine receptor. *Biophys. J.* **2007**, *93*, 2622–2634.
- (39) Nowak, M. W.; Gallivan, J. P.; Silverman, S. K.; Labarca, C. G.; Dougherty, D. A.; Lester, H. A. In vivo incorporation of unnatural amino acids into ion channels in *Xenopus* oocyte expression system. *Methods Enzymol.* **1998**, *293*, 504–529.
- (40) Cashin, A. L.; Torrice, M. M.; McMenimen, K. A.; Lester, H. A.; Dougherty, D. A. Chemical-scale studies on the role of a conserved aspartate in preorganizing the agonist binding site of the nicotinic acetylcholine receptor. *Biochemistry* **2007**, *46*, 630–639.
- (41) Saks, M. E.; Sampson, J. R.; Nowak, M. W.; Kearney, P. C.; Du, F.; Abelson, J. N.; Lester, H. A.; Dougherty, D. A. An engineered *Tetrahymena* tRNAGln for in vivo incorporation of unnatural amino acids into proteins by nonsense suppression. *J. Biol. Chem.* **1996**, *271*, 23169–23175.